Supporting Information

Krick *et al.* 10.1073/pnas.0801146105

SI Text

Animals and Microarray Procedures. As type 2 diabetes models we used male db/db (Leprdb/db) mice together with nondiabetic control db/m on C57BLKs/J background (Jackson Labs). As a type 1 diabetes model we used male and female Akita (C57B6J/Ins2Akita) mice together with nondiabetic control C57B6/J mice. As the chronic kidney disease mouse models, we used TGF beta transgenic animals (1). All animal protocols and procedures were approved by the IACUC at the Mount Sinai School of Medicine.

Apoptosis Detection. Apoptotic nuclei were detected using DAPI staining (1 μg/ml;10 min) in combination with a TUNEL labeling kit (Chemicon) and analyzed by fluorescence microscopy. Briefly, cells were plated on coverslips and treated when they reached 50% confluency. Cells were fixed with 4% PFA, permeabilized with 1% Triton, and stained with TUNEL according to the manufacturer's protocol. To exclude necrosis, cells were double labeled with propidium iodide. Cells were counted and the rate of apoptosis was determined by assessing the amount of apoptotic cells in a field of 50 (MCT) or 20 (HEK, MEFs) cells. For each individual experiment, we counted 10 fields per coverslip. To support the TUNEL staining, Annexin V/propidium iodide (PI) (BD Biosciences) staining was used. Briefly, cells were washed twice with cold PBS and resuspended in Annexin V/PI staining solution according to the manufacturer's protocol. Cells were incubated for 15 min at RT in the dark and analyzed by flow cytometry within 1 h. Emitted fluorescence was determined by using a BD FACSCanto (BD Biosciences). Flow cytometry data were analyzed using FACS Diva (BD Biosciences). Unstained cells were used as a control, and apoptotic rate was shown as a percentage increase of Annexin V/PI-positive cells.

Immunofluorescence and Immunoelectron Microscopy. Immunofluorescence staining was performed as described previously (2). Antibodies: anti-cytochrome *c* (BD PharMingen); anti-PMP70, anti-catalase, and DAPI (Sigma Aldrich); and Dolichos biflorus agglutinin (Vector). Fluorescent images were acquired by a Leica TCS SP confocal microscope. For immunogold labeling, ultrathin frozen sections of perfusion-fixed rat kidney were reacted with polyclonal Mpv17l antibody (1:30) overnight as described previously (3). The sections were analyzed using a Phillips EM 301 electron microscope.

Plasmid Constructs. The full-length cDNAs encoding for mouse l-Mpv17l (NM_033564), s-Mpv17l (BC037713) and Htr2A were created by RT-PCR using mouse kidney poly mRNA or an HtrA2 National Institutes of Health image clone (MGC: 5321861) as templates and were cloned into pEGFP-C1/N1 (BD Biosciences Clontech) and pFLAG 5a,b (Sigma–Aldrich) and pGEX expression vectors. All constructs were verified by DNA sequencing. The hybrid constructs of the Smac/DIABLO mitochondrial import signal and the mature form of HtrA2, as well as the HtrA2S306A mutant, were kindly provided by D. Vaux (La Trobe University, Melbourne, Australia).

GST-Binding Assays. GST pull-down studies from tissue and cell extracts were performed as reported previously (4). Mpv17l-GST fusion proteins were expressed in *E. coli* Bl21 (Stratagene) at 30°C. Bacterial lysates were incubated with glutathione agarose beads (Sigma–Aldrich) and rotated overhead for 1 h at 4°C. Kidney protein extracts were incubated with the GST-fusion proteins.

Detection of Activated Bax. Activated Bax was detected according to the protocol previously published by Chao *et al.* (5). Briefly, 293T cells were transfected with either control or Mpv17l construct for 24 h, stimulated with 1 μM antimycin A for 2 h and 24 h, and then lysed in 1% CHAPS buffer. Activated Bax was immunoprecipitated from lysates using the mouse monoclonal Bax-antibody (6A7; BD Biosciences) followed by immunoblotting for total Bax using a rabbit polyclonal anti-Bax antibody (Cell Technology).

Gene Silencing by Stable RNA Interference. The plasmid vector pSUPER containing a zeocin resistance cassette was used for stable expression of siRNA in MCT cells (6). The s-Mpv17l-specific insert was a 19 nt sequence (GATGTAAGCAATA-AAGCAC) corresponding to nt 36–54 of the mouse Mpv17l ORF, which is separated by a 9 nt noncomplementary spacer (TTCAAGAGA) from the reverse complement of the same 19 nt sequence. A control vector (pSUPER-control) was constructed using a 19 nt scrambled sequence with no significant homology to any mammalian gene sequence. MCT cells were transfected with 1 μg of siRNA plasmid. Seventy-two hours after transfection, stable transfectants were selected with 400 μg/ml Zeocin (Invitrogen). Clonal cell lines were selected and tested for Mpv17l expression by western blotting as described.

Generation of the Mpv17l Polyclonal Antibody. Rabbits were immunized with a peptide conjugated with keyhole limpet hemocyanin (KLH) corresponding to AA181–194 of Mpv17l (NP_291042; single-letter code CFLRRKEASDKSPEK) that is common for the long and the short isoform (Invitrogen). The antiserum was affinity purified with the corresponding peptide linked to Ultralink (Pierce) according to the manufacturer's instructions.

Tissue Extraction, Western Blotting, and Immunoprecipitation. Kidney tissue and cultured cells were lysed and subjected to 12% SDS/PAGE. The following primary antibodies were used for antigen detection: mouse monoclonal anti-GAPDH (Santa Cruz), rabbit polyclonal anti-HtrA2, and mouse anti-cytochrome *c* (PharMingen). For subcellular fractionation, cytosolic and mitochondrial fractions were prepared by selective plasma membrane permeabilization with digitonin as previously described (7). For coimmunoprecipitation of FLAG- and GFP-fusion proteins, 293T cells were cotransfected and harvested after 24 h as previously described (4).

1. Sanderson N, *et al.* (1995) Hepatic expression of mature transforming growth factor beta 1 in transgenic mice results in multiple tissue lesions. *Proc Natl Acad Sci USA* 92:2572–2576.
2. Susztak K, Ciccone E, McCue P, Sharma K, Bottinger EP (2005) Multiple metabolic hits converge on CD36 as novel mediator of tubular epithelial apoptosis in diabetic nephropathy. *PLoS Med* 2:e45.
3. Mundel TM, Heid HW, Mahuran DJ, Kriz W, Mundel P (1999) Ganglioside GM2-activator protein and vesicular transport in collecting duct intercalated cells. *J Am Soc Nephrol* 10:435–443.
4. Schwarz K, *et al.* (2001) Podocin, a raft-associated component of the glomerular slit diaphragm, interacts with CD2AP and nephrin. *J Clin Invest* 108:1621–1629.
5. Chao JR, *et al.* (2008) Hax1-mediated processing of HtrA2 by Parl allows survival of lymphocytes and neurons. *Nature* 452:98–102.
6. Brummelkamp TR, Bernards R, Agami R (2002) A system for stable expression of short interfering RNAs in mammalian cells. *Science* 296:550–553.
7. Adrain C, Creagh EM, Martin SJ (2001) Apoptosis-associated release of Smac/DIABLO from mitochondria requires active caspases and is blocked by Bcl-2. *EMBO J* 20:6627–6636.

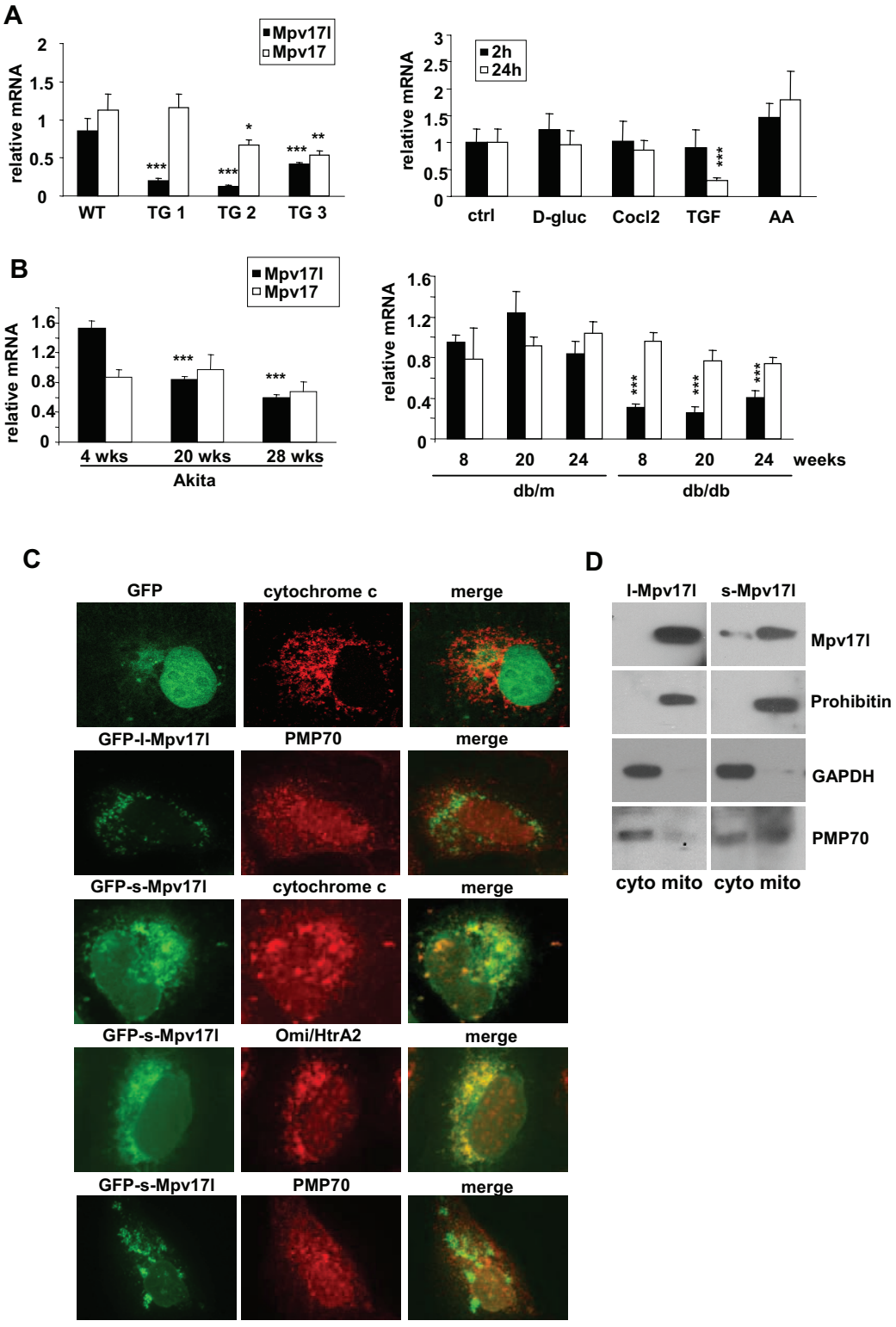

Fig. S1. Regulation of Mpv17l mRNA and localization of Mpv17l protein. (*A*) Bar graphs show average ± SEM of normalized, relative mRNA levels for Mpv17l and Mpv17 in whole kidneys of 4-week-old TGF β1 transgenic mice with kidney disease, compared with control mice and normalized, relative Mpv17l mRNA levels of MCT cells, exposed to different stimuli for 2 h and 24 h. (*B*) Bar graphs show average ± SEM of normalized, relative mRNA levels for Mpv17l and Mpv17 in whole kidneys of two diabetic mouse models (Akita: type 1 and db/db: type 2 mouse model) at different ages compared with control mice (C57BL/6 and db/m). Two mice were used at each age. Statistical analysis was performed by using Student's *t* test and ANOVA of three independent experiments with *, $P < 0.05$; **, $P < 0.01$; ***, $P < 0.005$. (*C*) COS-7 cells, transfected with GFP as a control vector, were stained with the mitochondrial marker anti-cytochrome *c* and visualized using confocal microscopy. To analyze possible colocalization with peroxisomes, GFP-l-Mpv17l-transfected COS-7 cells were stained with anti-Omi/HtrA2 and anti-PMP70. COS-7 cells, transfected with GFP-tagged s-Mpv17l were double labeled with anti-cytochrome *c*, anti-Omi/HtrA2 and anti-PMP70. (*D*) Representative immunoblot of Mpv17l protein levels showing subcellular fractions of extracts from 293T cells, transfected with either FLAG-l-Mpv17l or GFP-s-Mpv17l. GAPDH (cytosolic fraction) and prohibitin (mitochondrial fraction) protein levels, were used for equal loading. PMP70 protein levels are shown to indicate the distribution of the peroxisomes in the subcellular fractions.

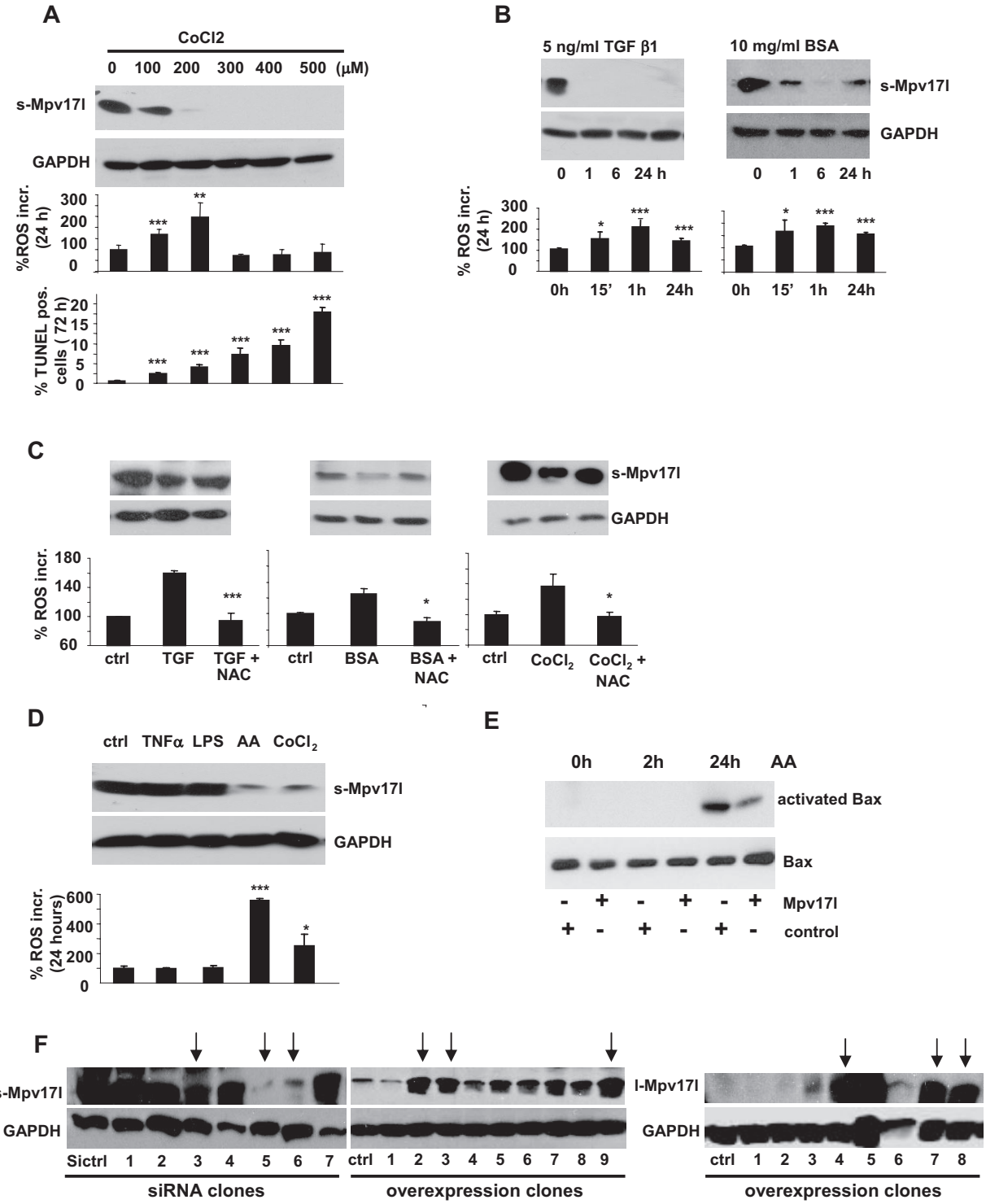

Fig. S2. Down-regulation of Mpv17l protein levels is associated with an increase of ROS generation and apoptosis in murine proximal tubular epithelial (MCT) cells exposed to a panel of extracellular ROS generators. (*A*) Mpv17l immunoblot, percentage ROS increase and apoptosis rate in MCT cells exposed to $CoCl_2$ as a stimulus mimicking hypoxia for 24 h at different concentrations as indicated. (*B*) Mpv17l immunoblot and bar graphs indicating percentage ROS increase of MCT cells exposed to transforming growth factor 1β (TGFβ1) and BSA at different time points as indicated. (*C*) Representative Mpv17l immunoblot and bar graphs indicating percentage ROS increase of MCT cells after 30 min preincubation with *N*-acetylcysteine (NAC; 1 mM) and subsequent exposure to TGFβ1, BSA, and $CoCl_2$. (*D*) Immunoblot showing Mpv17l protein levels and bar graphs showing average $\pm$ SEM of percentage ROS increase in MCT cells, treated for 24 h with tumor necrosis factor α (TNFα; 20 ng/ml), lipopolysacharide (LPS;100 μg/ml), and the complex III inhibitor antimycin A (1 μM) and $CoCl_2$ (200 μM). GAPDH levels were used for equal loading. Results are representative of three independent experiments. Statistical analysis was performed using Student's *t* test and ANOVA with *, $P < 0.05$; **, $P < 0.01$; ***, $P < 0.005$. (*E*) Representative immunoblot of activated Bax and Bax input in 293T cells, transfected with either control or Mpv17l and subsequent stimulation with antimycin A for 2 h and 24 h. (*F*) Representative Mpv17l immunoblot of cell lysates from different MCT cell clones, either stable transfected with a siRNA s-Mpv17l construct or a control scrambled siRNA construct and anti-Mpv17l immunoblot of MCT clones, stably overexpressing either the s-Mpv17l, l-Mpv17l isoform or the empty vector as control. The arrows indicate clones, which were used for further functional analysis. GAPDH levels were used for equal loading.

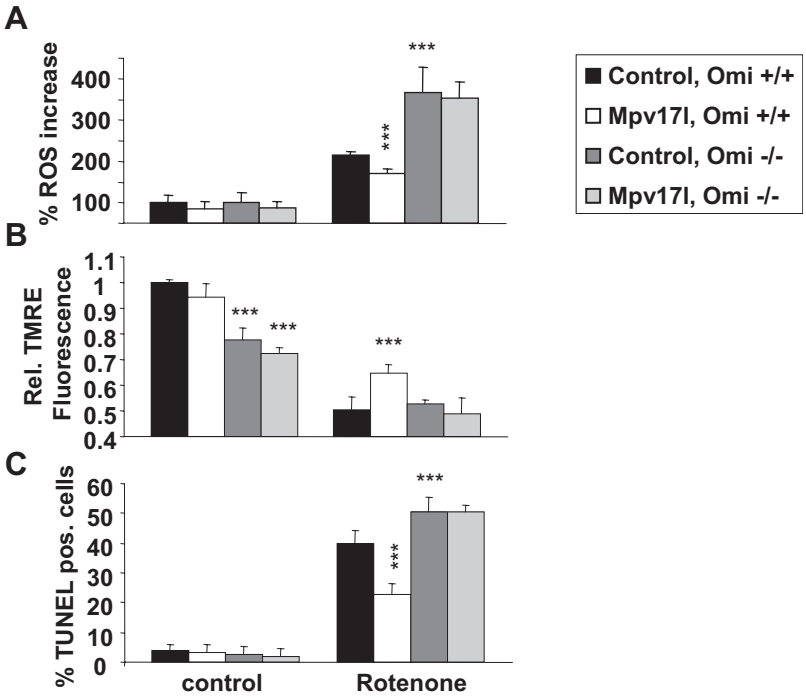

Fig. S3. HtrA2 is required for the protective role of Mpv17l in mitochondria. (*A*) Bar graphs showing average ± SEM of percent increase of mitochondrial superoxide levels, (*B*) the relative change of $\Delta\Psi_m$, and (*C*) the rate of apoptosis of wild type and HtrA2 −/− MEFs, transfected with either FLAG-control or FLAG-l-Mpv17l and stimulated with 25 μM Rotenone for 27 h. Results are representative data from three independent experiments. Statistical analysis was performed by using Student's *t* test and ANOVA with *, $P < 0.05$; **, $P < 0.01$; ***, $P < 0.005$.

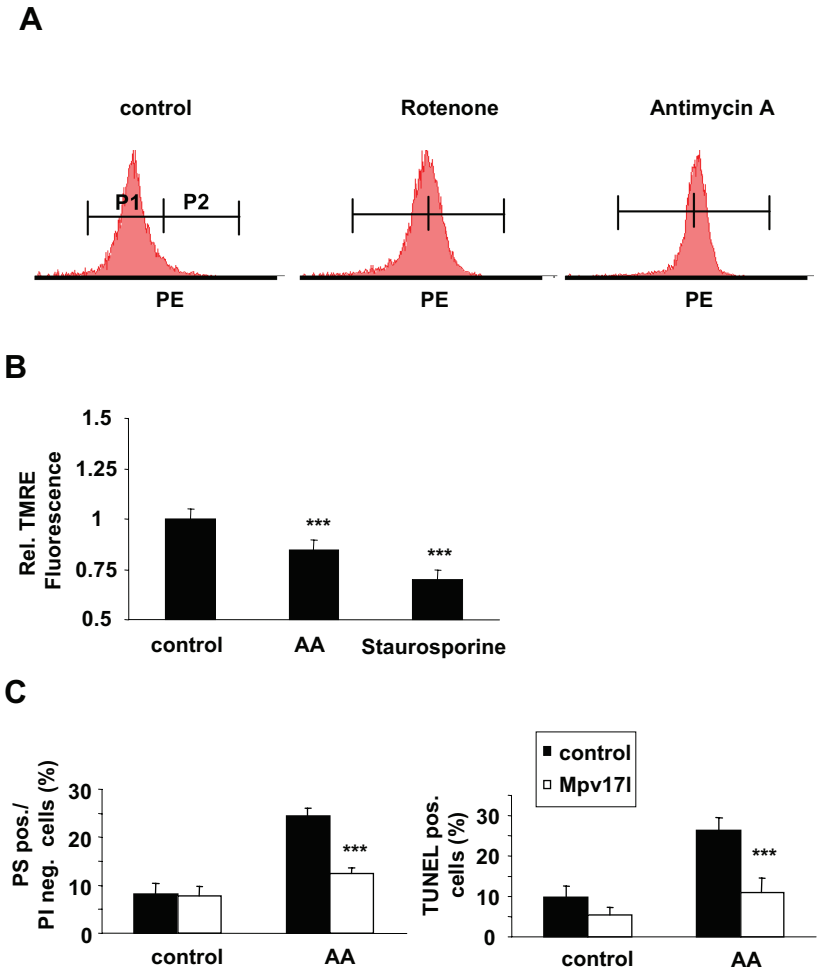

Fig. S4. Control stimuli for evaluation of ROS analysis and comparison of TUNEL with Annexin V (phosphatidyl serine, PS)/PI exposure. (*A*) Histograms depicting results of flowcytometric MitoSOX analysis, with MCT cells, stimulated with rotenone and antimycin A for 24 h, compared with control cells. The *x* axis represents the MitoSOX fluorescence. (*B*) MCT cells were stimulated with antimycin A (1 μM) for 12 h and staurosporine (0.5 μM) for 30 min. Results show decrease of TMRE fluorescence, analyzed by FACS and compared with untreated cells. (*C*) 293T cells were transfected with either a control plasmid or Mpv17l and stimulated with antimycin A for 24 h. PS/PI was measured by FACS scan and TUNEL-positive cells/field of 20 cells were counted using fluorescence microscopy. Results are representative data from three independent experiments. Statistical analysis was performed using Student's *t* test and ANOVA with $*$, $P < 0.05$; $**$, $P < 0.01$; $***$, $P < 0.005$.